Uplink Performance of Wideband Massive MIMO With One-Bit ADCs

Christopher Mollén, Junil Choi, Erik G. Larsson, *Fellow, IEEE*, and Robert W. Heath, Jr., *Fellow, IEEE*

***Abstract*— Analog-to-digital converters (ADCs) stand for a significant part of the total power consumption in a massive multiple-input multiple-output (MIMO) base station. One-bit ADCs are one way to reduce power consumption. This paper presents an analysis of the spectral efficiency of single-carrier and orthogonal-frequency-division-multiplexing (OFDM) transmission in massive MIMO systems that use one-bit ADCs. A closed-form achievable rate, i.e., a lower bound on capacity, is derived for a wideband system with a large number of channel taps that employ low-complexity linear channel estimation and symbol detection. Quantization results in two types of error in the symbol detection. The circularly symmetric error becomes Gaussian in massive MIMO and vanishes as the number of antennas grows. The amplitude distortion, which severely degrades the performance of OFDM, is caused by variations between symbol durations in received interference energy. As the number of channel taps grows, the amplitude distortion vanishes and OFDM has the same performance as single-carrier transmission. A main conclusion of this paper is that wideband massive MIMO systems work well with one-bit ADCs.**

***Index Terms*— Channel estimation, equalization, OFDM, one-bit ADCs, wideband massive MIMO.**

I. Introduction

ONE-BIT Analog-to-Digital Converters (ADCs) are the least power consuming devices to convert analog signals into digital [1]. The use of one-bit ADCs also simplifies the analog front end, e.g., automatic gain control (AGC) becomes trivial because it only considers the sign of the input signal. Such radically coarse quantization has been suggested for use in massive Multiple-Input Multiple-Output (MIMO) base stations, where the large number of radio chains makes high resolution ADCs a major power consumer. Recent studies have shown that the performance loss due to the coarse quantization of one-bit ADCs can be overcome with a large number of receive antennas [2]–[5].

Several recent papers have proposed specific symbol detection algorithms for massive MIMO with low-resolution ADCs. For example, a near-maximum-likelihood detector for one-bit quantized signals was proposed in [3], while [4] and [6] studied the use of linear detection. In [7], it was proposed to use a mix of one-bit and high resolution ADCs, which was shown to give a performance similar to an unquantized system. The proposed algorithms, however, focused only on frequency-flat channels.

Maximum-likelihood channel estimation for frequency-flat MIMO channels with one-bit ADCs was studied in [8]. It was found that the quality of the estimates depends on the set of orthogonal pilot sequences used. This is contrary to unquantized systems, where any set of orthogonal pilot sequences gives the same result. Closed-loop channel estimation with dithering and bursty pilot sequences was proposed for the single-user frequency-selective channel in [9]. It is not apparent that bursty pilot sequences are optimal and no closed-form expression for their performance was derived. In [10]–[12], message passing algorithms were proposed that improve the estimation of sparse channels. Our paper, in contrast, studies general non-sparse channels.

Most previous work on massive MIMO with one-bit ADCs has focused on narrowband systems with frequency-flat channels, e.g., [3]–[8]. Since quantization is a nonlinear operation on the time-domain signal, there is no straightforward way to extend these results to wideband systems, in which the channel is frequency selective. Some recent work has proposed equalization and channel estimation algorithms for wideband systems [13]–[15]. In [13], an iterative Orthogonal-Frequency-Division-Multiplexing (OFDM) based equalization and channel estimation method was proposed. However, the method is only shown to work for long pilot sequences of length $N_{\mathrm{d}}K$ (N_{d} the number of subcarriers, K the number of users). In contrast, our method only requires pilots of length μKL ($L \ll N_{\mathrm{d}}$ is the number of channel taps), where $\mu = 1$ yields an acceptable performance in many cases. Our method thus allows for a more efficient use of the coherence interval for actual data transmission. In [14], a message passing algorithm for equalization of single-carrier signals and a linear least-squares method for channel estimation were proposed. The detection algorithm proposed in our paper is linear in the quantized signals and the channel estimation method is based on linear minimum-mean-square-error (LMMSE) estimation, which has the advantage of performing relatively well

Manuscript received February 25, 2016; revised July 26, 2016; accepted October 3, 2016. Date of publication October 19, 2016; date of current version January 6, 2017. This work was supported in part by the European Union Seventh Framework Programme under Grant ICT-619086 through MAMMOET, in part by the Swedish Research Council (Vetenskapsrådet), in part by the National Science Foundation under Grant NSF-CCF-1527079, and in part by the ICT R&D program of MSIP/IITP [2016 (B0717-16-0002)]. The associate editor coordinating the review of this paper and approving it for publication was P. A. Martin. (*Corresponding author: Junil Choi.*)

C. Mollén and E. G. Larsson are with the Department of Electrical Engineering, Linköping University, 581 83 Linköping, Sweden (e-mail: christopher.mollen@liu.se; erik.g.larsson@liu.se).

J. Choi is with the Department of Electrical Engineering, Pohang University of Science and Technology, Pohang 37673, South Korea (e-mail: junil@postech.ac.kr).

R. W. Heath, Jr. is with the Wireless Networking and Communications Group, The University of Texas at Austin, Austin, TX 78712 USA (e-mail: rheath@utexas.edu).

Color versions of one or more of the figures in this paper are available online at http://ieeexplore.ieee.org.

Digital Object Identifier 10.1109/TWC.2016.2619343

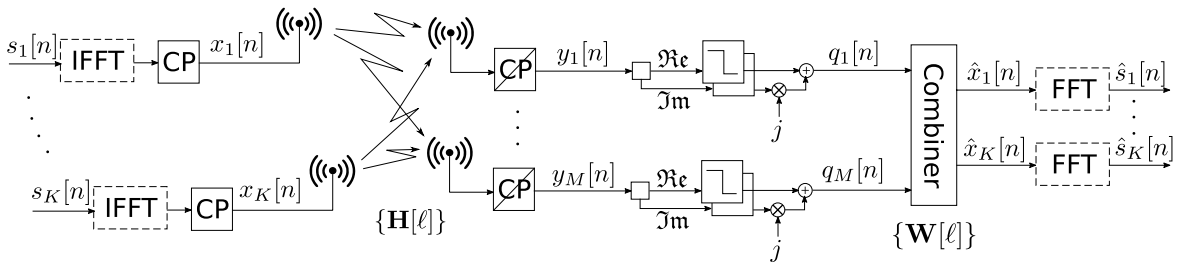

Fig. 1. System model for the massive MIMO uplink, both for single-carrier (without IFFT and FFT) and OFDM transmission.

independently of the noise variance. The use of a mix of low and high-resolution ADCs was also studied for frequency-selective single-user channels with perfect channel state information in [15]. However, the mixed ADC architecture increases hardware complexity, in that an ADC switch is required. Furthermore, it is not clear that the computational complexity of the designs in [13]–[15] is low enough for real-time symbol detection, especially in wideband systems where the sampling rate is high.

In this paper, we study a massive MIMO system with one-bit ADCs and propose to apply to the quantized signals low-complexity linear combiners for symbol detection and LMMSE channel estimation. These are the same techniques that previously have been suggested for unquantized massive multiuser MIMO [16] and that have proven possible to implement in real time [17]. Linear receivers for signals quantized by one-bit ADCs have not been studied for frequency-selective channels before.

Without any simplifying assumptions on the quantization distortion, we derive an achievable rate for single-carrier and OFDM transmission in the proposed system, where the channel is estimated from pilot data and the symbols are detected with linear combiners. A frequency-selective channel, in which the taps are Rayleigh fading and follow a general power delay profile, is assumed. When the number of channel taps grows large, the achievable rate is derived in closed-form for the maximum-ratio and zero-forcing combiners (MRC, ZFC). The rate analysis shows that simple linear receivers become feasible in wideband massive MIMO systems, where the performance loss compared to an unquantized system is approximately 4 dB. In many system setups, the performance of the quantized system is approximately 60–70% of the performance of the unquantized system at data rates around 2 bpcu. The loss can be made smaller, if longer pilot sequences can be afforded.

We also show that the performance of OFDM, without any additional signal processing, is the same as the performance of single-carrier transmission in wideband systems with a large number of channel taps. As was also noted in [18], the quantization error of the symbol estimates consists of two parts: one amplitude distortion and one circularly symmetric distortion, whose distribution is close to Gaussian. While the amplitude distortion causes significant intersymbol interference in OFDM, it can easily be avoided in single-carrier transmission. We show that the amplitude distortion vanishes when the number of taps grows. Therefore only the circularly symmetric noise, which affects single-carrier and OFDM transmission in the same way, is present in wideband systems with many taps. Hence, frequency selectivity is beneficial for linear receivers in massive MIMO because it reduces the quantization error and makes it circularly symmetric and additive. Results in [5] indicate that the capacity of quantized MIMO channels grows faster with the number of receive antennas at high signal-to-noise ratio (SNR) than the rate of the linear combiners. In a frequency-flat channel, where near-optimal detection becomes computationally feasible, a nonlinear symbol detection algorithm, e.g., [3], [14], would therefore be better than linear detectors, especially at a high SNR, where the linear ZFC fails to suppress all interference in the quantized system, even with perfect channel state information.

The most related work appeared in [19] and [20], where achievable rates for massive MIMO with one-bit ADCs and low-resolution ADCs for frequency-flat channels were investigated. In [19] an approximation was given for the achievable rate of a MRC system with low-resolution ADCs (one-bit ADCs being a special case) for a Rayleigh fading channel. The study showed a discrepancy between the approximation and the numerically obtained rate of one-bit ADCs [19, Fig. 2], which was left unexplained. In [20], an approximation of an achievable rate for Ricean fading frequency-flat channels (of which Rayleigh fading is a special case) was derived. Neither [19] nor [20] mentioned that quantization distortion might combine coherently and result in amplitude distortion and neither mentioned the dependence of the rate on the number of channel taps.

Parts of this work has been presented at [21], where the derivation of the achievable rate for MRC, a special case, was outlined. Channel estimation with fixed pilot lengths (equal to KL, i.e., with *pilot excess factor* 1) was also studied. This paper is more general and complete: generic linear combiners are studied, the detailed derivation of the achievable rate is shown and the effects of different pilot lengths are analyzed.

Paper disposition: The massive MIMO uplink with one-bit ADCs is presented in Section II. The quantization of one-bit ADCs is studied in Section III. Then the channel estimation is explained in Section IV. The uplink transmission is explained and analyzed in Section V. Finally, we present numerical results in Section VI and draw our conclusion in Section VII. The program code used in the numerical part can be found at [22].

II. System Model

We consider the massive MIMO uplink in Figure 1, where the base station is equipped with M antennas and there

are K single-antenna users. All signals are modeled in complex baseband and are uniformly sampled at the Nyquist rate with perfect synchronization. Because of these assumptions, the front-end depicted in Figure 1 has been simplified accordingly. Since the received signal is sampled at the Nyquist rate, there is no intermediate oversampled step before the matched receive filter (not in Figure 1), which thus has to be an analog filter. Note that the one-bit ADC itself does not require any AGC—a dynamic control loop with variable attenuators and amplifiers that precisely adjusts the input voltage to conventional ADCs to avoid clipping and to efficiently make use of the whole dynamic range that the ADC has to offer. Whereas one-bit ADCs has no need for this kind of fine tuning of their input voltage, the analog receive filter, which probably would be an active filter, might require some kind of mechanism to regulate its input voltage to avoid being overdriven. Such a mechanism would be simple to implement in comparison to the AGC of a conventional ADC and could possibly be combined with the low-noise amplifier [23].

At symbol duration n, base station antenna m receives:

$$y_m[n] \triangleq \sum_{k=1}^{K} \sum_{\ell=0}^{L-1} \sqrt{P_k} g_{mk}[\ell] x_k[n-\ell] + z_m[n], \tag{1}$$

where $x_k[n]$ is the transmit signal from user k, whose power $\mathbb{E}\big[|x_k[n]|^2\big] = 1$, P_k is the transmit power of user k and $z_m[n] \sim \mathcal{CN}(0, N_0)$ is a random variable that models the thermal noise of the base station hardware. It is assumed that $z_m[n]$ is identically and independently distributed (IID) over n and m and independent of all other variables. We assume that the L-tap impulse response $\{g_{mk}[\ell]\}$ of the channel between user k and antenna m can be written as the product of the small-scale fading $h_{mk}[\ell]$ and the large-scale fading $\sqrt{\beta_k}$:

$$g_{mk}[\ell] = \sqrt{\beta_k} h_{mk}[\ell]. \tag{2}$$

The small-scale fading has to be estimated by the base station. Its mean $\mathbb{E}[h_{mk}[\ell]] = 0$ and variance are *a priori* known:

$$\mathbb{E}\big[|h_{mk}[\ell]|^2\big] = p[\ell], \quad \forall \ell, \tag{3}$$

where $p[\ell]$ is the power delay profile of the channel, for which

$$\sum_{\ell=0}^{L-1} p[\ell] = 1. \tag{4}$$

In practice, the power delay profile depends on the propagation environment and has to be estimated, e.g., like in [24], where the power delay profile is estimated without additional pilots. The base station is also assumed to know the large-scale fading β_k, which generally changes so slowly over time that an accurate estimate is easy to obtain in most cases. The signal-to-noise ratio (SNR) is defined as

$$\mathsf{SNR}_k \triangleq \frac{P_k}{N_0} \sum_{\ell=1}^{L-1} \mathbb{E}[|g_{mk}[\ell]|^2] = \frac{\beta_k P_k}{N_0}. \tag{5}$$

In a wideband system, the number of channel taps L can be large—on the order of tens. For example, a system that uses 15 MHz of bandwidth over a channel with 1 μs of maximum excess delay, which corresponds to a moderately frequency-selective channel, has $L = 15$ channel taps. The Extended Typical Urban Model [25] has a maximum excess delay of 5 μs, leading to $L = 75$ taps.

Upon reception, the in-phase and quadrature signals are separately sampled, each by identical one-bit ADCs, to produce:

$$q_m[n] \triangleq \frac{1}{\sqrt{2}} \operatorname{sign}\big(\mathfrak{Re}(y_m[n])\big) + j \frac{1}{\sqrt{2}} \operatorname{sign}\big(\mathfrak{Im}(y_m[n])\big). \tag{6}$$

We assume that the threshold of the quantization is zero. Other thresholds can allow for better amplitude recovery when the interference and noise variance is small compared to the power of the desired signal [7], [26]. A small improvement in data rate can be obtained at low SNR when a non-zero threshold is paired with the optimal symbol constellation, see [27], where the SISO channel is studied. Since we study a multiuser system, where the interuser interference is high, we do not expect any significant performance improvement from a non-zero threshold. The scaling of the quantized signal is arbitrary but chosen such that $|q_m[n]| = 1$.

Two transmission modes are studied: single-carrier with frequency-domain equalization and OFDM transmission. We observe the transmission for a block of N symbols. At symbol duration n, user k transmits

$$x_k[n] = \begin{cases} s_k[n], & \text{if single-carrier} \\ \dfrac{1}{\sqrt{N}} \displaystyle\sum_{\nu=0}^{N-1} s_k[\nu] e^{j2\pi n\nu/N}, & \text{if OFDM,} \end{cases} \tag{7}$$

where $s_k[n]$ is the n-th data symbol. We assume that the symbols have zero-mean and unit-power, i.e., $\mathbb{E}\big[s_k[n]\big] = 0$ and $\mathbb{E}\big[|s_k[n]|^2\big] = 1$ for all k, n. The users also transmit a cyclic prefix that is $L-1$ symbols long:

$$x_k[n] = x_k[N+n], \quad -L < n < 0, \tag{8}$$

so that the input–output relation in (1) can be written as a multiplication in the frequency-domain, after the cyclic prefix has been discarded:

$$\mathsf{y}_m[\nu] = \sum_{k=1}^{K} \sqrt{\beta_k P_k} \mathsf{h}_{mk}[\nu] \mathsf{x}_k[\nu] + \mathsf{z}_m[\nu], \tag{9}$$

where

$$\mathsf{x}_k[\nu] \triangleq \frac{1}{\sqrt{N}} \sum_{n=0}^{N-1} x_k[n] e^{-j2\pi n\nu/N} \tag{10}$$

$$\mathsf{y}_m[\nu] \triangleq \frac{1}{\sqrt{N}} \sum_{n=0}^{N-1} y_m[n] e^{-j2\pi n\nu/N} \tag{11}$$

$$\mathsf{h}_{mk}[\nu] \triangleq \sum_{\ell=0}^{L-1} h_{mk}[\ell] e^{-j2\pi \ell\nu/N} \tag{12}$$

and $\mathsf{z}_m[\nu] \sim \mathcal{CN}(0, N_0)$ IID is the unitary Fourier transform of the thermal noise.

III. Quantization

In this section, some properties of the quantization of one-bit ADCs are derived. These results are used later in the channel estimation and the system analysis.

We define the quantization distortion as

$$e_m[n] \triangleq q_m[n] - \rho y_m[n], \tag{13}$$

where the scaling factor ρ is chosen to minimize the error variance $E \triangleq \mathbb{E}\big[|e_m[n]|^2\big]$, which is minimized by the Wiener solution:

$$\rho = \frac{\mathbb{E}\big[y_m^*[n] q_m[n]\big]}{\mathbb{E}\big[|y_m[n]|^2\big]}. \tag{14}$$

Note that the distribution of $e_m[n]$ depends on the distribution of the received signal $y_m[n]$ in a nonlinear way due to (6) and that $e_m[n]$ is uncorrelated to $y_m[n]$ due to the choice of ρ because of the orthogonality principle.

We define the expected received power given all transmit signals:

$$\begin{aligned} P_{\mathrm{rx}}[n] &\triangleq \mathbb{E}\big[|y_m[n]|^2 \mid \{x_k[n]\}\big] \\ &= N_0 + \sum_{k=1}^{K} \beta_k P_k \sum_{\ell=0}^{L-1} p[\ell] \big|x_k[n-\ell]\big|^2, \end{aligned} \tag{15}$$

and the average received power:

$$\bar{P}_{\mathrm{rx}} \triangleq \mathbb{E}\big[|y_m[n]|^2\big] = N_0 + \sum_{k=1}^{K} \beta_k P_k. \tag{16}$$

When the number of channel taps L in (15) is large, the two powers $P_{\mathrm{rx}}[n]$ and $\bar{P}_{\mathrm{rx}}$ are close to equal. This is formalized in the following lemma.

Lemma 1: Given a sequence of increasingly long power delay profiles $\{p_L[\ell]\}_{L=1}^{\infty}$ and a constant $\gamma \in \mathbb{R}$ such that $\max_\ell p_L[\ell] < \gamma/L$, for all lengths L, then

$$P_{\mathrm{rx}}[n] \xrightarrow{\text{a.s.}} \bar{P}_{\mathrm{rx}}, \quad L \to \infty, \qquad \forall n. \tag{17}$$

Proof: According to the law of large numbers and the Kolmogorov criterion [28, eq. (7.2)],

$$\sum_{\ell=0}^{L-1} p_L[\ell] \big|x_k[n-\ell]\big|^2 \xrightarrow{\text{a.s.}} \mathbb{E}\Big[\big|x_k[n-\ell]\big|^2\Big] = 1, \quad L \to \infty. \tag{18}$$

Thus, the inner sum in (15) tends to one as the number of channel taps grows. ∎

Because of the cyclic prefix, the block length N cannot be shorter than L. Therefore, it was assumed that N grew together with L in the proof of Lemma 1. As we will see later, the convergence can be fast, so the left-hand side in (17) is well approximated by its limit also for L much shorter than usual block lengths N.

Remark 1: Note that the sum over k in (15) also results in an averaging effect when the number of users K is large. The relative difference between the expected received power given all transmit signals and its mean $|P_{\mathrm{rx}}[n] - \bar{P}_{\mathrm{rx}}|/P_{\mathrm{rx}}[n]$ becomes small, not only with increasing L, but also with increasing K if there is no dominating user, i.e., some user k for which $\beta_k P_k \gg \beta_{k'} P_{k'}, \forall k' \neq k$. In practice, power control is done and most $\beta_k P_k$ will be of similar magnitude. The expected received power given all transmit signals is thus closely approximated by its average also in narrowband systems with a large number of users and no dominating user.

The next lemma gives the scaling factor and the variance of the quantization distortion.

Lemma 2: If the fading is IID Rayleigh, i.e., $h_{mk}[\ell] \sim \mathcal{CN}(0, p[\ell])$ for all m, k and ℓ, then the scaling factor defined in (14) is given by

$$\rho = \sqrt{\frac{2}{\pi}} \frac{\mathbb{E}\Big[\sqrt{P_{\mathrm{rx}}[n]}\Big]}{\bar{P}_{\mathrm{rx}}} \to \sqrt{\frac{2}{\pi \bar{P}_{\mathrm{rx}}}}, \quad L \to \infty, \tag{19}$$

and the quantization distortion has the variance

$$E = 1 - \rho^2 \bar{P}_{\mathrm{rx}} \to 1 - \tfrac{2}{\pi}, \quad L \to \infty. \tag{20}$$

Proof: See Appendix A. ∎

We see that the error variance in (20) would equal its limit if $P_{\mathrm{rx}}[n] = \bar{P}_{\mathrm{rx}}$ and $\rho^2 = \frac{2}{\pi \bar{P}_{\mathrm{rx}}}$. That is the reason the limit coincides with the mean-squared error of one-bit quantization in [29] and what is called the distortion factor of one-bit ADCs in [30].

The following corollary to Lemma 2 gives the limit of the relative quantization distortion variance, which is defined as

$$Q \triangleq \frac{E}{|\rho|^2}. \tag{21}$$

Corollary 1: The relative quantization distortion variance in a wideband system approaches

$$Q \to Q' \triangleq \bar{P}_{\mathrm{rx}} \Big(\frac{\pi}{2} - 1\Big), \quad L \to \infty. \tag{22}$$

Note that $Q \geq Q'$, because Jensen's inequality says that $\rho \leq \sqrt{\frac{2}{\pi \bar{P}_{\mathrm{rx}}}}$ is smaller than its limit in (19) for all L, since the square root is concave. This means that the variance of the quantization distortion is smaller in a wideband system, where the number of taps L is large, than in a narrowband system.

If there is no quantization, the variance of the quantization error $E = 0$ and thus the relative quantization distortion $Q = Q' = 0$. This allows us to use the expressions derived in the following sections to analyze the unquantized system as a special case.

IV. Channel Estimation

In this section, we will describe a low-complexity channel estimation method. In doing so, we assume that the uplink transmission is divided into two blocks: one with length $N = N_{\mathrm{p}}$ pilot symbols for channel estimation and one with length $N = N_{\mathrm{d}}$ symbols for data transmission. The two blocks are disjoint in time and studied separately. It is assumed, however, that the channel is the same for both blocks, i.e., that the channel is block fading and that both blocks fit within the same coherence time.

We define K orthogonal pilot sequences of length N_{p} as:

$$\phi_k[\nu] \triangleq \begin{cases} 0, & (\nu \mod K) + 1 \neq k \\ \sqrt{\frac{K}{N_{\mathrm{p}}}} e^{j\theta_k[\nu]}, & (\nu \mod K) + 1 = k, \end{cases} \tag{23}$$

where $\theta_k[\nu]$ is a phase that is known to the base station. During the training period, user k transmits the signal that, in the frequency domain, is given by

$$\boldsymbol{x}_k[\nu] = \sqrt{N_{\mathrm{p}}} \phi_k[\nu]. \tag{24}$$

The received signal (9) is then

$$y_m[\nu] = \sum_{k=1}^{K} \sqrt{\beta_k P_k N_{\mathrm{p}}} h_{mk}[\nu]\phi_k[\nu] + z_m[\nu] \tag{25}$$

$$= \sqrt{\beta_{k'} P_{k'} K} h_{mk'}[\nu] e^{j\theta_{k'}[\nu]} + z_m[\nu], \tag{26}$$

where $k' \triangleq (\nu \mod K) + 1$, in the last step, is the index of the user whose pilot $\phi_{k'}[\nu]$ is nonzero at tone ν. By rewriting the time-domain quantized signal using (13), we compute the quantized received signal in the frequency domain as

$$q_m[\nu] \triangleq \frac{1}{\sqrt{N_{\mathrm{p}}}} \sum_{n=0}^{N_{\mathrm{p}}-1} q_m[n] e^{-j2\pi n\nu/N_{\mathrm{p}}} \tag{27}$$

$$= \rho y_m[\nu] + \underbrace{\frac{1}{\sqrt{N_{\mathrm{p}}}} \sum_{n=0}^{N_{\mathrm{p}}-1} e_m[n] e^{-j2\pi n\nu/N_{\mathrm{p}}}}_{\triangleq e_m[\nu]} \tag{28}$$

$$= \rho\sqrt{\beta_{k'} P_{k'} K} h_{mk'}[\nu] e^{j\theta_{k'}[\nu]} + \rho z_m[\nu] + e_m[\nu]. \tag{29}$$

The sequence $\{q_m[\nu K + k - 1],\ \nu = 0, \ldots, \frac{N_p}{K} - 1\}$ is thus a phase-rotated and noisy version of the frequency-domain channel of user k, sampled with period $F = K$.

Because the time-domain channel $h_{mk}[\ell] = 0$ for all $\ell \notin [0, L-1]$, the sampling theorem says that, if the sampling period satisfies

$$F \leq \frac{N_{\mathrm{p}}}{L}, \tag{30}$$

it is enough to know the samples $\{h_{mk}[\nu F + k - 1],\ \nu = 0, \ldots, \frac{N_{\mathrm{p}}}{F} - 1\}$ of the channel spectrum to recover the time-domain channel:

$$h_{mk}[\ell] = \frac{F}{N_{\mathrm{p}}} \sum_{n=0}^{\frac{N_{\mathrm{p}}}{F}-1} h_{mk}[nF + k - 1] e^{j2\pi\ell(nF+k-1)/N_{\mathrm{p}}}. \tag{31}$$

Thus, if the number of pilot symbols satisfies $N_{\mathrm{p}} \geq KL$, then (30) is fulfilled and the following observation of the channel tap $h_{mk}[\ell]$ can be made through an inverse Fourier transform of the received samples that belong to user k:

$$h'_{mk}[\ell] \triangleq \sqrt{\frac{K}{N_{\mathrm{p}}}} \sum_{\nu=0}^{\frac{N_{\mathrm{p}}}{K}-1} q_m[\nu K + k - 1] e^{j2\pi\ell(\nu K+k-1)/N_{\mathrm{p}}} e^{-j\theta_k[\nu K+k-1]} \tag{32}$$

$$= \rho\sqrt{\beta_k P_k K}\sqrt{\frac{K}{N_{\mathrm{p}}}} \sum_{\nu=0}^{\frac{N_{\mathrm{p}}}{K}-1} h_{mk}[\nu K + k - 1] e^{j2\pi\ell(\nu K+k-1)/N_{\mathrm{p}}} + \underbrace{\rho\sqrt{\frac{K}{N_{\mathrm{p}}}} \sum_{\nu=0}^{\frac{N_{\mathrm{p}}}{K}-1} z_m[\nu K + k - 1] e^{j2\pi\ell(\nu K+k-1)/N_{\mathrm{p}}} e^{-j\theta_k[\nu K+k-1]}}_{\triangleq z'_{mk}[\ell]} + \underbrace{\sqrt{\frac{K}{N_{\mathrm{p}}}} \sum_{\nu=0}^{\frac{N_{\mathrm{p}}}{K}-1} e_m[\nu K + k - 1] e^{j2\pi\ell(\nu K+k-1)/N_{\mathrm{p}}} e^{-j\theta_k[\nu K+k-1]}}_{\triangleq e'_{mk}[\ell]} \tag{33}$$

$$= \rho\sqrt{\beta_k P_k N_{\mathrm{p}}} h_{mk}[\ell] + \rho z'_{mk}[\ell] + e'_{mk}[\ell]. \tag{34}$$

In the first step (33), $q_m[\nu]$ is replaced by the expression in (29). Then, in (34), the relation in (31) is used to rewrite the first sum as the time-domain channel impulse response. We note that the Fourier transform is unitary and therefore $z'_{mk}[\ell] \sim \mathcal{CN}(0, N_0)$ is independent across m, k, ℓ and $\mathbb{E}\big[|e'_{mk}[\ell]|^2\big] = \mathbb{E}\big[|e'_{mk}[\ell]|^2\big] = E$.

We use the LMMSE estimate of the channel, which is given by

$$\hat{h}_{mk}[\ell] \triangleq h'_{mk}[\ell] \frac{\mathbb{E}\big[h^*_{mk}[\ell] h'_{mk}[\ell]\big]^*}{\mathbb{E}\big[|h'_{mk}[\ell]|^2\big]} \tag{35}$$

$$= h'_{mk}[\ell] \frac{\rho p[\ell]\sqrt{\beta_k P_k N_{\mathrm{p}}}}{\rho^2 p[\ell]\beta_k P_k N_{\mathrm{p}} + \rho^2 N_0 + E} \tag{36}$$

and whose variance is $\mathbb{E}\big[|\hat{h}_{mk}[\ell]|^2\big] = c_k[\ell]p[\ell]$, where

$$c_k[\ell] \triangleq \frac{p[\ell]\beta_k P_k N_{\mathrm{p}}}{p[\ell]\beta_k P_k N_{\mathrm{p}} + N_0 + Q}. \tag{37}$$

The error $\epsilon_{mk}[\ell] \triangleq h_{mk}[\ell] - \hat{h}_{mk}[\ell]$ is uncorrelated to the channel estimate and has variance

$$\mathbb{E}\big[|\epsilon_{mk}[\ell]|^2\big] = \big(1 - c_k[\ell]\big) p[\ell]. \tag{38}$$

In the frequency domain, the channel estimate is given by

$$\hat{h}_{mk}[\nu] \triangleq \sum_{\ell=0}^{L-1} \hat{h}_{mk}[\ell] e^{-j2\pi\nu\ell/N_{\mathrm{d}}}, \quad \nu = 0, \ldots, N_{\mathrm{d}} - 1, \tag{39}$$

the estimation error $\varepsilon_{mk}[\nu] \triangleq h_{mk}[\nu] - \hat{h}_{mk}[\nu]$ and their variances:

$$\mathbb{E}\big[|\hat{h}_{mk}[\nu]|^2\big] = \sum_{\ell=0}^{L-1} c_k[\ell]p[\ell] \triangleq c_k \tag{40}$$

$$\mathbb{E}\big[|\varepsilon_{mk}[\nu]|^2\big] = 1 - c_k. \tag{41}$$

The variance of the channel estimate c_k will be referred to as the *channel estimation quality*.

We define the *pilot excess factor* as $\mu \triangleq \frac{N_{\mathrm{p}}}{KL} \geq 1$. Because $c_k \to 1$ as $\mu \to \infty$, the quality of the channel estimation in the quantized system can be made arbitrary good by increasing μ. Since the pilots have to fit within the finite coherence time of the channel however, the *channel estimation quality* will be limited in practice. To get a feeling for how large practical *pilot excess factors* can be, we consider an outdoor channel with Doppler spread $\sigma_\nu = 400$ Hz and delay spread $\sigma_\tau = 3$ µs and symbol duration T. The coherence time of this channel is approximately $N_{\mathrm{c}} \approx 1/(\sigma_\nu T)$ symbol durations and the number of taps $L \approx \sigma_\tau / T$. The pilots sequence will thus fit if $N_{\mathrm{p}} \leq N_{\mathrm{c}}$, i.e., only *pilot excess factors* such that $\mu \leq 1/(K\sigma_\nu\sigma_\tau) \approx 830/K$ are feasible in this channel. Because of the finite coherence time of the practical channel, we will study the general case of finite μ.

To compare the *channel estimation quality* of a quantized wideband system to that of the corresponding unquantized

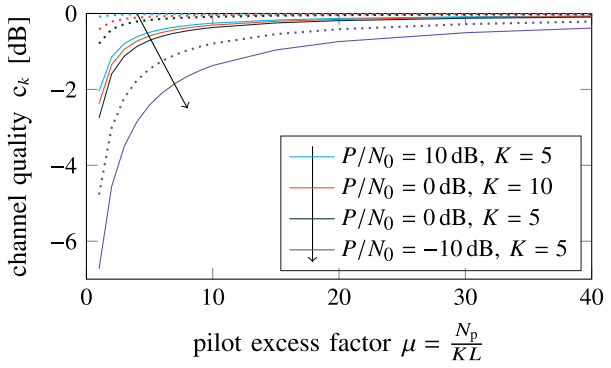

Fig. 2. The *channel estimation quality* for the quantized system with one-bit ADCs in solid lines and for the unquantized system in dotted lines for a uniform power delay profile $p[\ell] = 1/L$.

system, we define

$$c_k\big|_{Q=0,\mu=\mu_0} \triangleq \sum_{\ell=0}^{L-1} \frac{p^2[\ell]\beta_k P_k \mu_0 KL}{p[\ell]\beta_k P_k \mu_0 KL + N_0} \tag{42}$$

$$c_k\big|_{Q=\bar{P}_{\rm rx}(\frac{\pi}{2}-1),\mu=\mu_{\rm q}} \triangleq \sum_{\ell=0}^{L-1} \frac{p^2[\ell]\beta_k P_k \mu_{\rm q} KL}{p[\ell]\beta_k P_k \mu_{\rm q} KL + N_0 + \bar{P}_{\rm rx}(\frac{\pi}{2}-1)} \tag{43}$$

$$\Delta(\mu_0, \mu_{\rm q}) \triangleq \frac{c_k\big|_{Q=0,\mu=\mu_0}}{c_k\big|_{Q=\bar{P}_{\rm rx}(\frac{\pi}{2}-1),\mu=\mu_{\rm q}}}, \tag{44}$$

where μ_0 is the excess factor of the unquantized system, $\mu_{\rm q}$ is that of the one-bit ADC system and $\Delta(\mu_0, \mu_{\rm q})$ the quality ratio. If this ratio is one, the channel estimates of the two systems are equally good. Under the assumption that $\beta_k P_k = P$, $\forall k$, and $p[\ell] = 1/L$, $\forall \ell$, the difference in *channel estimation quality* always is less than 2 dB when the excess factors $\mu_{\rm q} = \mu_0 = \mu$ are the same:

$$\Delta(\mu, \mu) \leq \frac{\pi}{2} \approx 2\text{dB}, \tag{45}$$

Further, it can be seen that $\Delta(1, 1) = \pi/2$ and that $\Delta(\mu, \mu)$ is decreasing in μ. This can be seen in Figure 2, where the *channel estimation quality* c_k is plotted for different SNRs P/N_0, where $\beta_k P_k = P$ for all k. It can be seen that the power loss due to channel estimation is small in many system setups—in the order of -2 dB.

Remark 2: To increase the length of the training period and to increase the transmit power of the pilot signal would give the same improvement in *channel estimation quality* in the unquantized system. Because the orthogonality of the pilots is broken by the quantization, this is not true for the quantized system, which can be seen in (37), where Q is a function of only the transmit power. This is the reason the phases $\theta_k[n]$ are introduced: non-constant phases allow for *pilot excess factors* $\mu > 1$. Note that, with constant phases (assume $\theta_k[n] = 0$ without loss of generality), the pilot signal transmitted during the training period (26) is sparse in the time domain:

$$x_k[n] = \begin{cases} \sqrt{\mu L}, & \text{if } n = \nu\mu L + k - 1, \quad \nu \in \mathbb{Z} \\ 0, & \text{otherwise,} \end{cases} \tag{46}$$

i.e., it is zero in intervals of width $\mu L - 1$. If $\mu > 1$ there are intervals, in which nothing is received. The estimate is then based on few observations, each with relatively high SNR. By choosing the phases such that they are no longer constant, for example according to a uniform distribution $\theta_k[\nu] \sim \text{unif}[0, 2\pi)$, the pilot signal is no longer sparse in the time domain. The estimate is then based on many observations, each with relatively low SNR. Increasing the number of low-SNR observations is a better way to improve the quality of the channel estimate than increasing the SNR of a few observations in a quantized system. Furthermore, the limits in Lemma 2 are only valid if the received power $P_{\rm rx}[n]$ becomes constant as $L \to \infty$, which is not the case when there are intervals, in which nothing is received.

V. Uplink Data Transmission

In this section, one block of $N = N_{\rm d}$ symbols of the uplink data transmission is studied. Practical linear symbol detection based on the estimated channel is presented and applied to the massive MIMO system with one-bit ADCs. The distribution of the symbol estimation error due to quantization and how OFDM is affected is also analyzed. Finally, the performance is evaluated by deriving an achievable rate for the system.

A. Receive Combining

Upon reception, the base station combines the received signals using an FIR filter with transfer function $\mathsf{w}_{km}[\nu]$ and impulse response

$$w_{km}[\ell] \triangleq \frac{1}{N_{\rm d}} \sum_{\nu=0}^{N_{\rm d}-1} \mathsf{w}_{km}[\nu] e^{j2\pi\nu\ell/N_{\rm d}}, \quad \ell = 0, \ldots, N_{\rm d} - 1 \tag{47}$$

to obtain an estimate of the time-domain transmit signal:

$$\hat{x}_k[n] \triangleq \sum_{m=1}^{M} \sum_{\ell=0}^{N_{\rm d}-1} w_{km}[\ell] q_m\big[[n-\ell]_{N_{\rm d}}\big], \tag{48}$$

where $[n]_{N_{\rm d}} \triangleq n \bmod N_{\rm d}$, and, equivalently, of the frequency-domain transmit signals

$$\hat{\mathsf{x}}_k[\nu] \triangleq \sum_{m=1}^{M} \mathsf{w}_{km}[\nu] \mathsf{q}_m[\nu], \tag{49}$$

where $\mathsf{q}_m[\nu]$ is the Fourier transform of the quantized signals. The symbol estimate of user k is then obtained as

$$\hat{s}_k[n] = \begin{cases} \hat{x}_k[n], & \text{if single-carrier} \\ \hat{\mathsf{x}}_k[n], & \text{if OFDM.} \end{cases} \tag{50}$$

The combiner weights are derived from the estimated channel matrix $\hat{\mathbf{H}}[\nu]$, whose (m, k)-th element is $\hat{h}_{mk}[\nu]$. Three common combiners are the Maximum-Ratio, Zero-Forcing, and Regularized Zero-Forcing Combiners (MRC, ZFC, RZFC):

$$\mathbf{W}'[\nu] = \begin{cases} \hat{\mathbf{H}}^{\rm H}[\nu], & \text{if MRC} \\ \big(\hat{\mathbf{H}}^{\rm H}[\nu]\hat{\mathbf{H}}^{\rm H}[\nu]\big)^{-1}\hat{\mathbf{H}}^{\rm H}[\nu], & \text{if ZFC} \\ \big(\hat{\mathbf{H}}^{\rm H}[\nu]\hat{\mathbf{H}}^{\rm H}[\nu] + \lambda \mathbf{I}_K\big)^{-1}\hat{\mathbf{H}}^{\rm H}[\nu], & \text{if RZFC,} \end{cases} \tag{51}$$

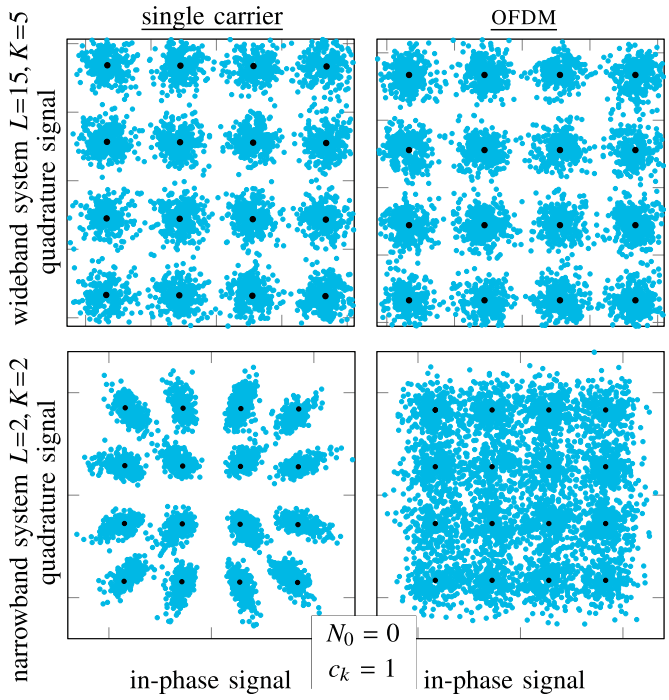

Fig. 3. Symbol estimates after one-bit quantization and ZFC in a massive MIMO base station with 128 antennas that serves K users over an L-tap channel. Even without thermal noise $N_0 = 0$ (the received powers $\beta_k P_k = 1$ for all users k) and perfect channel state information ($c_k = 1$), ZFC cannot suppress all interference due to the quantization. The amplitude distortion, which manifests itself as oblong clouds pointing away from the origin in the lower left narrowband system, disturbs the orthogonality of the OFDM symbols in the lower right system and causes additional estimation error. The amplitude distortion is negligible in the single-carrier wideband system (the quantization distortion forms circular, not oblong, clouds), which makes the estimates of the single-carrier and OFDM systems at the top equally good.

where λ is a regularization factor. The energy scaling of the combiner weights is arbitrary; for convenience, it is chosen as follows:

$$\mathbf{w}_{km}[\nu] = \frac{1}{\sqrt{\alpha_k}} \mathbf{w}'_{km}[\nu], \tag{52}$$

where $\alpha_k \triangleq \sum_{m=1}^{M} \mathbb{E}\big[|\mathbf{w}'_{km}[\nu]|^2\big]$ and $\mathbf{w}'_{km}[\nu]$ is element (k, m) of the matrix $\mathbf{W}'[\nu]$. In practice, RZFC would always be preferred because of its superior performance. The two other combiners, MRC and ZFC, are included for their mathematical tractability. The MRC also has an implementational advantage over the other combiners—it is possible to do most of its signal processing locally at the antennas in a distributed fashion.

Remark 3: As was noted in [31], the energy of the impulse response in (47) is generally concentrated to a little more than L of the taps for the receive combiners defined in (51). For example, the energy is concentrated to exactly L taps for MRC, whose impulse response is the time-reversed impulse response of the channel. Because, in general, $L \ll N_{\mathrm{d}}$, a shorter impulse response simplifies the implementation of the receive combiner.

B. Quantization Error and Its Effect on Single-Carrier and OFDM Transmission

In this section, we show that the estimation error due to quantization consists of two parts: one amplitude distortion and one circularly symmetric. The amplitude distortion degrades the performance of the OFDM system more than it does the single-carrier system. In a wideband system however, the amplitude distortion is negligible and OFDM works just as well as single-carrier transmission.

If $\{h_{mk}[\ell]\}$ is a set of uncorrelated variables, the quantization distortion can be written as:

$$e_m[n] = \sum_{k=1}^{K} \sum_{\ell=0}^{L-1} \frac{\mathbb{E}\big[h^*_{mk}[\ell] e_m[n] \,\big|\, \{x_k[n]\}\big]}{\mathbb{E}\big[|h_{mk}[\ell]|^2\big]} h_{mk}[\ell] + d_m[n], \tag{53}$$

where $d_m[n]$ is the residual error with the smallest variance. The sum in (53) can be seen as the LMMSE estimate of $e_m[n]$ based on $\{h_{mk}[\ell]\}$ conditioned on $x_k[n]$ and the second term as the estimation error, which is uncorrelated to the channel $\{h_{mk}[\ell]\}$. The following lemma gives the coefficients in this sum.

Lemma 3: If $h_{mk}[\ell] \sim \mathcal{CN}(0, p[\ell])$, the normalized conditional correlation

$$\frac{\mathbb{E}\big[h^*_{mk}[\ell] e_m[n] \,\big|\, \{x_k[n]\}\big]}{\mathbb{E}\big[|h_{mk}[\ell]|^2\big]} = \sqrt{\frac{2}{\pi}} x_k[n-\ell]\tau[n] \tag{54}$$

$$\xrightarrow{\text{a.s.}} 0, \quad L \to \infty, \tag{55}$$

where

$$\tau[n] \triangleq \frac{\sqrt{P_{\mathrm{rx}}[n]}}{P_{\mathrm{rx}}[n]} - \frac{\mathbb{E}\Big[\sqrt{P_{\mathrm{rx}}[n]}\Big]}{\bar{P}_{\mathrm{rx}}}. \tag{56}$$

Proof: See Appendix B. ∎

By assuming that the channel taps are uncorrelated to each other and by using (54) in (53), the quantization distortion becomes:

$$e_m[n] = \sqrt{\frac{2}{\pi}} \tau[n] \bar{y}_m[n] + d_m[n], \tag{57}$$

where the noise-free received signal is

$$\bar{y}_m[n] \triangleq \sum_{k=1}^{K} \sum_{\ell=0}^{L-1} h_{mk}[\ell] x_k[n-\ell]. \tag{58}$$

By using (13) to write $q_m[n] = \rho y_m[n] + e_m[n]$, the symbol estimate of the receive combiner in (48) can be written as:

$$\hat{x}_k[n] = \sum_{m=1}^{M} \sum_{\ell=0}^{N_{\mathrm{d}}-1} w_{km}[\ell](\rho y_m[n-\ell] + e_m[n-\ell]). \tag{59}$$

Therfore, we define the error due to quantization as

$$e'_k[n] \triangleq \sum_{m=1}^{M} \sum_{\ell=0}^{N_{\mathrm{d}}-1} w_{km}[\ell] e_m[n-\ell] \tag{60}$$

$$= \sqrt{\frac{2}{\pi}} \sum_{m=1}^{M} \sum_{\ell=0}^{N_{\mathrm{d}}-1} w_{km}[\ell] \tau[n-\ell] \bar{y}_m[n-\ell] + \sum_{m=1}^{M} \sum_{\ell=0}^{N_{\mathrm{d}}-1} w_{km}[\ell] d_m[n-\ell]. \tag{61}$$

The first term in (61) contains the noise-free received signal $\bar{y}_m[n]$ and will result in an amplitude distortion, i.e., error that contains a term that is proportional to the transmit signal $x_k[n]$

or the negative transmit signal $-x_k[n]$ (depending on the sign of $\tau[n]$).

When the number of channel taps goes to infinity, three things happen. (i) The amplitude distortion that contains $\tau[n]$ vanishes because $\tau[n] \to 0$ as $L \to \infty$ according to Lemma 3. (ii) The variance of the error approaches

$$\mathbb{E}\big[|e'_k[n]|^2\big] \to \mathbb{E}\big[|d_m[n]|^2\big] = E, \quad L \to \infty. \tag{62}$$

(iii) The number of terms in the second sum in (61) grows with L, as noted in Remark 3. Therefore the sum converges in distribution to a Gaussian random variable according to the central limit theorem:

$$e'_k[n] \xrightarrow{\text{dist.}} \mathcal{CN}(0, E), \quad L \to \infty. \tag{63}$$

The rate at which the amplitude distortion vanishes depends on the rate of convergence in (17), i.e., the amplitude distortion is small in systems, in which $P_{\text{rx}}[n]$ is close to $\bar{P}_{\text{rx}}$ for all n.

The effect of the quantization can be seen in Figure 3, where the symbol estimates $\hat{s}_k[n]$ after receive combining are shown for four systems. All other sources of estimation error (except quantization) have been removed: there is no thermal noise, no error due to imperfect channel state knowledge and ZFC is used to suppress interuser interference. In narrowband systems, there is coherent amplitude distortion that increases the variance of the symbol error due to quantization and that will not disappear by increasing the number of antennas. We see that the impact of the amplitude distortion is more severe in the OFDM system, where the it gives rise to intersymbol interference, than in the single-carrier system, where distinct, albeit non-symmetric, clusters still are visible. In wideband systems, the amplitude distortion has vanished and there is no visible difference in the distribution of the quantization distortion of the symbol estimates for single-carrier and OFDM transmission. This phenomenon was studied in detail in [18], where it was found that the symbol distortion due to quantization, in general, results in a nonlinear distortion of the symbol amplitudes. If, however, the effective noise (interference plus thermal noise) is large compared to the power of the desired received signal, then the amplitude distortion vanishes and the estimated symbol constellation is a scaled and noisy version of the transmitted one. This happens when the number of channel taps or the number of users is large.

In a wideband massive MIMO system with one-bit ADCs and linear combiners, there is thus no amplitude distortion and the error due to quantization can be treated as additional AWGN (Additive White Gaussian Noise). As a consequence, the transmission can be seen as the transmission over several parallel frequency-flat AWGN channels. Over such channels, the performance of different symbol constellations can be evaluated using standard methods, such as minimum Euclidean distance relative to the noise variance. Specifically, arbitrary QAM constellations can be used as well as OFDM. Detailed results with practical symbol constellations can be found in [4].

C. Achievable Rate

In this section, we derive an achievable rate for the uplink of the quantized one-bit ADC massive MIMO system. The achievable rate, in the limit of a large number of channel taps L, is then derived in closed form. As will be seen, this limit closely approximates the achievable rate of a wideband system also with practically large L.

Using the orthogonality principle, the estimate $\hat{\boldsymbol{x}}_k[\nu]$ can be written as a sum of two terms

$$\hat{\boldsymbol{x}}_k[\nu] = a\boldsymbol{x}_k[\nu] + \zeta_k[\nu], \tag{64}$$

where $\zeta_k[\nu]$ is the residual error. By choosing the factor $a \triangleq \mathbb{E}\big[\boldsymbol{x}_k^*[\nu]\hat{\boldsymbol{x}}_k[\nu]\big]$, the variance of the error $\zeta_k[\nu]$ is minimized and the error becomes uncorrelated to the transmit signal $\boldsymbol{x}_k[\nu]$. The variance of the error term is then

$$\mathbb{E}\big[|\zeta_k[\nu]|^2\big] = \mathbb{E}\big[|\hat{\boldsymbol{x}}_k[\nu]|^2\big] - \big|\mathbb{E}\big[\boldsymbol{x}_k^*[\nu]\hat{\boldsymbol{x}}_k[\nu]\big]\big|^2. \tag{65}$$

If we denote the distribution of the transmit signal $\boldsymbol{x}_k[\nu]$ by f_X, an achievable rate can be derived in the following manner. The capacity is lower bounded by:

$$\begin{aligned} C &= \max_{\{f_X:\mathbb{E}[|\boldsymbol{x}_k[\nu]|^2]\le 1\}} I(\boldsymbol{x}_k[\nu]; \hat{\boldsymbol{x}}_k[\nu]) && (66)\\ &\ge I(\boldsymbol{x}_k[\nu]; \hat{\boldsymbol{x}}_k[\nu])\big|_{\boldsymbol{x}_k[\nu]\sim\mathcal{CN}(0,1)} && (67)\\ &\ge R_k \triangleq \log_2\left(1 + \frac{\big|\mathbb{E}\big[\boldsymbol{x}_k^*[\nu]\hat{\boldsymbol{x}}_k[\nu]\big]\big|^2}{\mathbb{E}\big[|\hat{\boldsymbol{x}}_k[\nu]|^2\big] - \big|\mathbb{E}\big[\boldsymbol{x}_k^*[\nu]\hat{\boldsymbol{x}}_k[\nu]\big]\big|^2}\right). && (68)\end{aligned}$$

In (67), the capacity is bounded by assuming that the transmit signals are Gaussian. In (68), we use results from [32, eq. (46)] to lower bound the mutual information. The expectations are over the small-scale fading and over the symbols. The derived rate is thus achievable by coding over many channel realizations. In hardened channels [33], however, the rate is achievable for any single channel realization with high probability.

Because the Fourier transform is unitary, the corresponding rate for single-carrier transmission is the same as (68), which can be proven by showing that $\mathbb{E}\big[x_k^*[n]\hat{x}_k[n]\big] = \mathbb{E}\big[\boldsymbol{x}_k^*[\nu]\hat{\boldsymbol{x}}_k[\nu]\big]$.

To gain a better understanding of the achievable rate, we will partition the estimate $\hat{\boldsymbol{x}}_k[\nu]$ into components that are uncorrelated to the transmit signal $\boldsymbol{x}_k[\nu]$. By writing the channel as $\boldsymbol{h}_{mk}[\nu] = \hat{\boldsymbol{h}}_{mk}[\nu] + \varepsilon_{mk}[\nu]$ the received signal becomes

$$\boldsymbol{y}_m[\nu] = \sum_{k=1}^{K} \sqrt{c_k\beta_k P_k}\,\bar{\boldsymbol{y}}_{mk}[\nu] + \boldsymbol{u}_m[\nu] + \boldsymbol{z}_m[\nu], \tag{69}$$

where

$$\bar{\boldsymbol{y}}_{mk}[\nu] \triangleq \frac{1}{\sqrt{c_k}}\hat{\boldsymbol{h}}_{mk}[\nu]\boldsymbol{x}_k[\nu], \tag{70}$$

$$\boldsymbol{u}_m[\nu] \triangleq \sum_{k=1}^{K} \sqrt{\beta_k P_k}\,\varepsilon_{mk}[\nu]\boldsymbol{x}_k[\nu]. \tag{71}$$

Just like the time-domain estimate in (59), the frequency-domain estimate of the transmit signal can be partitioned by

rewriting the quantized signal using the relation in (13):

$$\hat{x}_k[\nu] = \sum_{m=1}^{M} w_{km}[\nu]\Big(\rho \sum_{k'=1}^{K} \sqrt{c_{k'}\beta_{k'}P_{k'}}\,\bar{y}_{mk'}[\nu] + \rho u_m[\nu] + \rho z_m[\nu] + e_m[\nu]\Big) \tag{72}$$

$$= \rho \sum_{k'=1}^{K} \sqrt{c_{k'}\beta_{k'}P_{k'}} \underbrace{\sum_{m=1}^{M} w_{km}[\nu]\bar{y}_{mk'}[\nu]}_{\triangleq \hat{x}'_{kk'}[\nu]} + \rho \underbrace{\sum_{m=1}^{M} w_{km}[\nu]u_m[\nu]}_{\triangleq u'_k[\nu]} + \rho \underbrace{\sum_{m=1}^{M} w_{km}[\nu]z_m[\nu]}_{\triangleq z'_k[\nu]} + \underbrace{\sum_{m=1}^{M} w_{km}[\nu]e_m[\nu]}_{=e'_k[\nu]}. \tag{73}$$

The terms $\{\hat{x}'_{kk'}[\nu]\}$ can further be split up in a part that is correlated to the transmit signal and a part that is not:

$$\hat{x}'_{kk'}[\nu] = \alpha_{kk'}x_k[\nu] + i_{kk'}[\nu], \tag{74}$$

where $\alpha_{kk'} \triangleq \mathbb{E}\big[x_k^*[\nu]\hat{x}'_{kk'}[\nu]\big]$ and $i_{kk'}[\nu]$ is the interference that is uncorrelated to $x_k[\nu]$. It is seen that $\alpha_{kk'} = 0$ for all $k' \neq k$, i.e., that only the term $\hat{x}'_{kk}[\nu]$ is correlated to the transmit signal $x_k[\nu]$. We denote the gain $G_k \triangleq |\alpha_{kk}|^2$ and the interference variance $I_{kk'} \triangleq \mathbb{E}\big[|i_{kk'}[\nu]|^2\big]$. Since they do not depend on the quality of the channel estimates nor on the quantization coarseness, they characterize the combiner that is used. In general, these characteristic parameters are determined numerically. Using results from random matrix theory, they were computed for MRC and ZFC in [34] and [35] for an IID Rayleigh fading channel $h_{mk}[\ell] \sim \mathcal{CN}(0, p[\ell])$:

$$G_k = \begin{cases} M \\ M-K, \end{cases} \qquad I_{kk'} = \begin{cases} 1, & \text{for MRC} \\ 0, & \text{for ZFC.} \end{cases} \tag{75}$$

With RZFC, the parameter λ can balance array gain and interference suppression to obtain characteristic parameters in between those of MRC and ZFC to maximize the SINR (Signal-to-Interference-and-Noise Ratio) of the symbol estimates that is given by the following theorem for wideband channels.

Theorem 1: When the small-scale fading coefficients are IID and $h_{mk}[\ell] \sim \mathcal{CN}\big(0, p[\ell]\big)$, the achievable rate R_k in (68) approaches

$$R_k \to R'_k, \quad L \to \infty, \tag{76}$$

where

$$R'_k \triangleq \log_2\left(1 + \frac{c_k\beta_k P_k G_k}{\sum_{k'=1}^{K} \beta_{k'}P_{k'}\big(1 - c_{k'}(1 - I_{kk'})\big) + N_0 + Q'}\right). \tag{77}$$

Proof: See Appendix C. ∎

From (75), we get the following corollary about MRC and ZFC.

Corollary 2: The achievable rates for MRC and ZFC systems, where $h_{mk}[\ell] \sim \mathcal{CN}(0, p[\ell])$ IID and when $L \to \infty$, are

$$R_{\text{MRC}} = \log_2\Big(1 + \frac{2}{\pi}\frac{c_k\beta_k P_k M}{N_0 + \sum_{k'=1}^{K}\beta_{k'}P_{k'}}\Big), \tag{78}$$

$$R_{\text{ZFC}} = \log_2\Big(1 + \frac{2}{\pi}\frac{c_k\beta_k P_k (M-K)}{N_0 + \sum_{k'=1}^{K}\beta_{k'}P_{k'}(1 - c_{k'}\frac{2}{\pi})}\Big). \tag{79}$$

Remark 4: By looking at the SINR of (77), we see that, whereas the numerator scales with G_k, which scales with M for MRC and ZFC, the variance of the quantization distortion Q' does not scale with M, just like the other noise terms (which was observed in [16] too). In a wideband system, quantization is thus a noncoherent noise source that disappears in the limit $M \to \infty$. Hence, arbitrary high rates are achievable by increasing the number of antennas, also in a system with one-bit ADCs.

For the unquantized MRC and ZFC, the achievable rates become:

$$R_{\text{MRC}_0} = \log_2\left(1 + \frac{c_k\beta_k P_k M}{N_0 + \sum_{k'=1}^{K}\beta_{k'}P_{k'}}\right) \tag{80}$$

$$R_{\text{ZFC}_0} = \log_2\left(1 + \frac{c_k\beta_k P_k (M-K)}{N_0 + \sum_{k'=1}^{K}\beta_{k'}P_{k'}(1 - c_{k'})}\right). \tag{81}$$

Note that c_k should be understood as the *channel estimation quality* of the unquantized system $c_k\big|_{Q=0}$; it is not the same as c_k in (78) and (79).

Remark 5: For quantized MRC with *pilot excess factor* μ_{q}, the SINR in (78) is a fraction

$$\frac{2}{\pi\,\Delta(\mu_0, \mu_{\text{q}})} \tag{82}$$

smaller than the SINR of the unquantized system in (80) with *pilot excess factor* μ_0 independently of the SNR. With equal *channel estimation quality* $\Delta(\mu_0, \mu_{\text{q}}) = 1$ the SINR loss is $2/\pi \approx -2$ dB. In light of (45), the SINR loss increases to -4 dB if both *pilot excess factors* $\mu_{\text{q}} = \mu_0 = 1$ and the receive powers $\beta_k P_k = P$ are the same from all users and the power delay profile $p[\ell] = 1/L$ for all ℓ. The same SINR loss is experienced in the quantized ZFC system at low SNR $\beta_k P_k/N_0$. At high SNR however, the performance of ZFC is greatly reduced as the interference is not perfectly suppressed. Even with perfect channel state information ($c_k = 1$), it is seen from the rate expression (79) that there is residual interference in the quantized system. This gives a rate ceiling, as was pointed out in for example [36], [37]. In [36] and [37], the reason for the incomplete interference suppression was imperfect channel state knowledge. In the quantized system, the reason is the distortion of the received signals. Whereas the rate of the unquantized ZFC system grows without bound as $P/N_0 \to \infty$ ($\beta_k P_k = P, \forall k$), the rate of the quantized system approaches the rate ceiling:

$$R_{\text{ZFC}} \to \log_2\left(1 + \frac{N_{\text{p}}(M-K)}{(\frac{\pi}{2} - 1)K(N_{\text{p}} + K)}\right), \quad \frac{P}{N_0} \to \infty. \tag{83}$$

Thus, one-bit ADCs with ZFC work well at low SNR, but incur a performance loss at high SNR. At high SNR, however, other imperfections than quantization also limit the performance of ZFC. For example, pilot contamination [16] results in a rate ceiling also in the unquantized system, which is not apparent

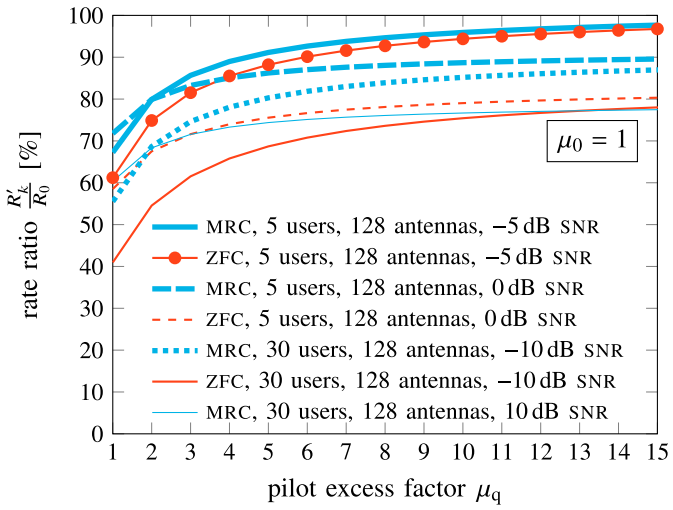

Fig. 4. Performance ratio R'_k/R_0 between the quantized and unquantized systems as a function of the *pilot excess factor* of the quantized system. The *pilot excess factor* of the unquantized system is $\mu_0 = 1$. All users have equal SNR $\beta_k P_k/N_0$.

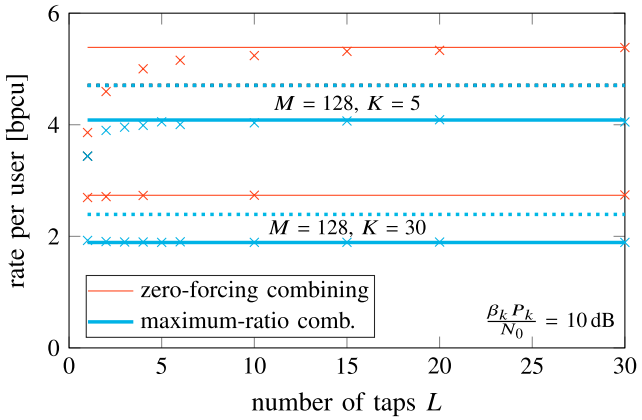

Fig. 5. The achievable rate R_k marked $\times$ and its limit R'_k drawn with a solid line for a system with 128 antennas that serves 5 and 30 users over an L-tap channel with Rayleigh fading taps. The dotted line shows the rate of the unquantized system with MRC. The rate of the unquantized ZFC is 10 bpcu for $K = 5$ and 9.9 bpcu for $K = 30$. The channel is known perfectly by the base station.

in our analysis. The performance loss at high SNR might therefore be smaller than predicted here.

Because of the similarities between the rate expressions of the quantized and unquantized systems, many of the properties of the unquantized massive MIMO system carry over to the one-bit quantized system. For example that ZFC performs poorly when the number of antennas M is close to the number of users K, i.e., when $M - K$ is small ($M \geq K$ for ZFC to exist). Similarly, quantization does not change the fact that the rate of MRC is higher than that of ZFC at low SNR, where array gain, which is larger for MRC than for ZFC ($2M/\pi$ compared to $2(M-K)/\pi$), is more important than interference suppression.

Earlier results showed that, with perfect channel state information, the capacity of a SISO channel [38] and a MIMO channel [39] decreases by a factor $2/\pi$ at low SNR when the signals are quantized by one-bit ADCs. Our results indicate that the rate expressions for the low-complexity detectors MRC and ZFC also decrease by a factor $2/\pi$ at low SNR when one-bit ADCs are used, as long as $\Delta(\mu_0, \mu_q) = 1$, i.e., as long as the channel state information is the same in the quantized and unquantized systems.

To compare the two systems, we let R_0 denote the achievable rate of the unquantized system that uses a fixed *pilot excess factor* $\mu_0 = 1$. The ratio R'_k/R_0 is drawn in Figure 4. We see that the quantized system achieves approximately 60–70 % of the unquantized rate with MRC in the studied systems. With ZFC, the ratio is around 60 % when there are 5 users but only 40 % with 30 users at low SNR. At high SNR, the ratio can be much lower, e.g., 20 % for 30 users at 10 dB SNR. Further the figure shows that the ratio can be improved by increasing the length of the pilot sequences in the quantized system. The largest improvement, however, is by going from $\mu_q = 1$ to $\mu_q = 2$. After that, the improvement saturates in most systems.

VI. Numerical Examples

In this section, we verify how close the limit R'_k in Theorem 1 is the achievable rate R_k in (68) for wideband systems with a finite number of channel taps L. The rate R_k is numerically evaluated for the massive MIMO system with one-bit ADCs described in Section II with the linear channel estimation and receive combining described in the Sections IV and V. As a way of comparing the quantized system to the unquantized, the number of extra antennas needed to make the quantized rate the same as the unquantized, while maintaining the same transmit power, is established. Such a comparison is sensible in a system where the number of users is fixed. If more users were available, a system with more antennas could potentially also serve more users and thus get a higher multiplexing gain.

The channel taps are modeled as IID Rayleigh fading and follow a uniform power delay profile, i.e., $h_{mk}[\ell] \sim \mathcal{CN}(0, 1/L)$. The large-scale fading is neglected and all received powers $\beta_k P_k/N_0$ are assumed to be equal for all users k in the first part of the study. This corresponds to doing a fair power control among the users, where the transmit power P_k is chosen proportional to $1/\beta_k$. Such a power control is possible to do since the users are assumed to know the large-scale fading. It is also desirable many times to ensure that all served users have similar SNR so that quality of service is uniformly good.

First, we study the convergence of the achievable rate R_k in (68) towards its limit by comparing R_k for finite L to the limit R'_k in (77) in Figure 5. It is seen that the limit R'_k is indeed an accurate approximation of the achievable rate R_k when the number of channel taps is large. For the system with 128 antennas and 5 users, the limit R'_k is close to R_k already at $L = 15$ taps, which corresponds to a moderately frequency-selective channel. For the system with 128 antennas and 30 users, however, the limit R'_k is a good approximation for R_k also in a narrowband scenario with $L = 1$. This immediate convergence was explained by Remark 1, where it was noted that the wideband approximation is valid also

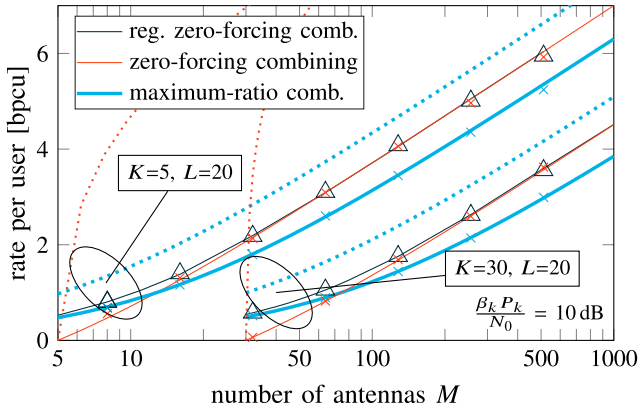

Fig. 6. Achievable rate R_k (marked $\times$ and $\triangle$), its limit R'_k (solid lines) and the rate R_k for the unquantized system (dotted lines) at high SNR $\beta_k P_k/N_0 = 10$ dB, $\forall k$, using the same number of pilot symbols. The channel taps are IID Rayleigh fading and estimated with $N_{\mathrm{p}} = KL$ pilot symbols. The curves for single-carrier and OFDM transmission coincide both for maximum-ratio and zero-forcing combining.

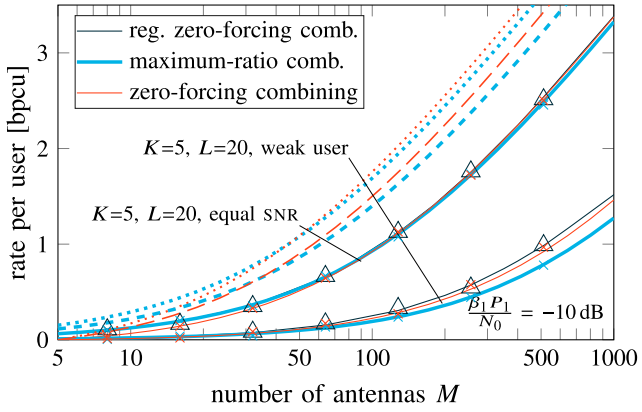

Fig. 7. Same setup as in Figure 6 except the SNR is low. For one set of curves, all users have the same SNR $\beta_k P_k/N_0 = -10$ dB. For the other, marked weak user, the studied user has -10 dB SNR while the interfering users have 0 dB SNR. The rate of the unquantized system is drawn with dotted lines for equal SNR and with dashed lines for the weak user.

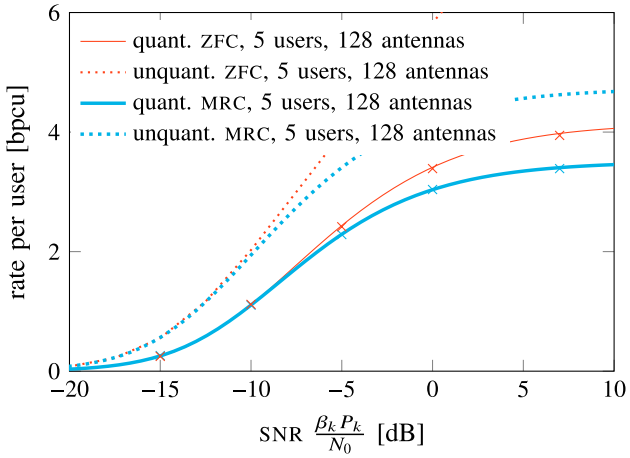

Fig. 8. Rate R'_k. All users have the same SNR. The channel is estimated with $N_{\mathrm{p}} = KL$ pilot symbols.

when the number of users is large and there is no dominant user.

The lower performance for small L for the case of 5 users in Figure 5 is caused by the amplitude distortion discussed in Section V-B. As the amplitude distortion disappears with more taps, the rate R_k increases. The improvement saturates when the amplitude distortion is negligible and the limit R'_k is a close approximation of R_k. This suggests that linear receivers for one-bit ADCs work better with frequency-selective channels than with frequency-flat channels and that wideband systems are beneficial when one-bit ADCs are used.

The rates of some wideband massive MIMO systems at high SNR $\beta_k P_k/N_0 = 10$ dB and low SNR -10 dB are shown for different numbers of base station antennas in Figures 6 and 7 respectively. We observe that the limit R'_k approximates the rate R_k well in all studied cases. Furthermore, we note that the quantized system needs 2.5 times ($\approx$4 dB) more antennas to ensure the same rate as the unquantized system with MRC, which was predicted in Remark 5. With ZFC at high SNR, the gap between the quantized and unquantized rates is much larger. At low SNR however, the gap is greatly decreased; then 2.6 times more antennas are needed in the quantized system to obtain the same performance as the unquantized system. The rate of RZFC is similar to MRC and ZFC, whichever is better for a given M; it is in part or fully hidden by the curves of MRC and ZFC. For this reason, only the quantized RZFC is included.

In Figure 7, we consider a user whose SNR is 10 dB weaker than the SNRs of the interfering users $\beta_k P_k/N_0 = 10\beta_1 P_1/N_0 = 0$ dB for $k = 2, 3, 4, 5$. This can happen if there is one user whose transmit power is limited for some practical reason or if a user happens to experience shadowing by the environment. The result is marked with "weak user" in Figure 6. We see that such a weak user gets a much lower rate than the case where all users have the same SNR. This is because of the increased interference that the weak user suffers. The gap between the unquantized system and the quantized system is larger for a weak user than for users with the same SNR as all the other users because the *channel estimation quality* is heavily degraded when the orthogonality of the pilots is lost in the quantization. For ZFC, 10.4 times more antennas are needed and for MRC 10.6 times, which should be compared to 2.6 and 2.5 times for equal SNR. Users that are relatively weak compared to interfering users should therefore be avoided in one-bit ADC systems, for example by proper user scheduling. In case weak users cannot be avoided, such users will have to obtain good channel estimates, either by longer pilot sequences or by increasing the transmit power of their pilots.

In Figure 8, the rate as a function of SNR is shown for some systems. It can be seen that the rate of the quantized systems is limited by a rate ceiling, as was indicated in (83). Around 70 % of the performance of the unquantized system can be achieved by the quantized system with MRC at -5 dB SNR, which gives approximately 2 bpcu. At the same SNR, ZFC achieves 60 % of the unquantized rate, which agrees with Figure 4. As observed, this performance loss can be compensated for by increasing the number of base station antennas. An increase of

antennas, however, would also lead to an increase in hardware complexity, cost and power consumption. Having in mind that one-bit ADCs at the same time greatly reduces these three practical issues, it is difficult to give a straightforward answer to whether one-bit ADCs are better, in some sense, than ADCs of some other resolution. A thorough future study of the receive chain hardware has to answer this question.

VII. Conclusion

We derived an achievable rate for a practical linear massive MIMO system with one-bit ADCs with estimated channel state information and a frequency-selective channel with IID Rayleigh fading taps and a general power delay profile. The derived rate is a lower bound on the capacity of a massive MIMO system with one-bit ADCs. As such, other nonlinear detection methods could perform better at the possible cost of increased computational complexity. The rate converges to a closed-form limit as the number of taps grows. We have shown in numerical examples that the limit approximates the achievable rate well also for moderately frequency-selective channels with finite numbers of taps.

A main conclusion is that frequency-selective channels are beneficial when one-bit ADCs are used at the base station. Such channels spread the received interference evenly over time, which makes the estimation error due to quantization additive and circularly symmetric. This makes it possible to use low-complexity receive combiners and low-complexity channel estimation for multiuser symbol detection. One-bit ADCs decrease the power consumption of the analog-to-digital conversion at a cost of an increased required number of antennas or reduced rate performance. At low to moderate SNR, approximately three times more antennas are needed at the base station to reach the same performance as an unquantized system when the channel is estimated by the proposed low-complexity channel estimation method.

The symbol estimation error due to quantization consists of two parts in a massive MIMO system: one amplitude distortion and one additive circularly symmetric Gaussian distortion. The amplitude distortion becomes negligible in a wideband system, which makes the implementation of OFDM straightforward. Since the error due to quantization is circularly symmetric Gaussian, systems that use OFDM are affected in the same way by one-bit quantizers as single-carrier systems, which means that many previous results for single-carrier systems carry over to OFDM systems.

By oversampling the received signal, it is possible that a better performance can be obtained than the one established by the achievable rate derived in this paper. Future research on massive MIMO with coarse quantization should focus on receivers that oversample the signal.

Appendix A
Proof of Lemma 2

From (14), the scaling factor is given by

$$\begin{aligned}\bar{P}_{\mathrm{rx}}\rho &= \mathbb{E}\big[y_m^*[n]q_m[n]\big] && (84)\\ &= \frac{1}{\sqrt{2}}\mathbb{E}\Big[\big(\mathfrak{Re}(y_m[n]) - j\,\mathfrak{Im}(y_m[n])\big)\\ &\quad\times\big(\mathfrak{Re}(y_m[n])\big| + \big|\mathfrak{Im}(y_m[n])\big|\\ &\quad + j\big(\mathfrak{Re}(y_m[n])\,\mathrm{sign}(\mathfrak{Im}(y_m[n]))\\ &\quad - \mathfrak{Im}(y_m[n])\,\mathrm{sign}(\mathfrak{Re}(y_m[n]))\big)\Big] && (85)\\ &= \sqrt{2}\mathbb{E}\Big[\mathbb{E}\Big[\big|\mathfrak{Re}(y_m[n])\big|\;\Big|\;\{x_k[n]\}\Big]\Big] && (86)\\ &= \mathbb{E}\left[\sqrt{\frac{2}{\pi}P_{\mathrm{rx}}[n]}\right]. && (87)\end{aligned}$$

In (85), the imaginary part of the expected value is zero, because $\mathfrak{Re}(y_m[n])$ and $\mathfrak{Im}(y_m[n])$ are IID and have zero mean. Further, by conditioning on the transmit signals, the inner expectation in (86) can be identified as the mean of a folded normal distributed random variable, which gives (87).

The error variance is derived as

$$\begin{aligned}\mathbb{E}\big[|e_m[n]|^2\big] &= \mathbb{E}\big[|q_m[n] - \rho y_m[n]|^2\big] && (88)\\ &= 1 - \rho^2\mathbb{E}\big[|y_m[n]|^2\big]. && (89)\end{aligned}$$

The limits in (19) and (20) follow directly from Lemma 1.

Appendix B
Proof of Lemma 3

Because they are functions of each other, the random variables $h_{mk}[\ell]$, $y_m[n]$, $e_m[n]$ form a Markov chain in that order. Therefore:

$$\begin{aligned}&\mathbb{E}\big[h_{mk}^*[\ell]e_m[n]\;\big|\;\{x_k[n]\}\big]\\ &\quad= \mathbb{E}\Big[\mathbb{E}\big[h_{mk}^*[\ell]e_m[n]\;\big|\;y_m[n]\big]\;\Big|\;\{x_k[n]\}\Big] && (90)\\ &\quad= \mathbb{E}\Big[\mathbb{E}\big[h_{mk}^*[\ell]\;\big|\;y_m[n]\big]\mathbb{E}\big[e_m[n]\mid y_m[n]\big]\;\Big|\;\{x_k[n]\}\Big] && (91)\\ &\quad= \frac{x_k[n-\ell]p[\ell]}{P_{\mathrm{rx}}[n]}\mathbb{E}\big[y_m^*[n](q_m[n] - \rho y_m[n])\;\big|\;\{x_k[n]\}\big] && (92)\\ &\quad= \frac{x_k[n-\ell]p[\ell]}{P_{\mathrm{rx}}[n]}\big(\mathbb{E}\big[y_m^*[n]q_m[n]\;\big|\;\{x_k[n]\}\big] - \rho P_{\mathrm{rx}}[n]\big) && (93)\\ &\quad= x_k[n-\ell]p[\ell]\left(\frac{\sqrt{\frac{2}{\pi}P_{\mathrm{rx}}[n]}}{P_{\mathrm{rx}}[n]} - \frac{\mathbb{E}\left[\sqrt{\frac{2}{\pi}P_{\mathrm{rx}}[n]}\right]}{\bar{P}_{\mathrm{rx}}}\right). && (94)\end{aligned}$$

In (92), we used the fact that the mean of a Gaussian variable conditioned on a Gaussian-noisy observation is the LMMSE estimate of that variable, i.e.,

$$\mathbb{E}\big[h_{mk}[\ell]\;\big|\;y_m[n],\{x_k[n]\}\big] = \frac{x_k^*[n-\ell]p[\ell]}{P_{\mathrm{rx}}[n]}y_m[n]. \quad (95)$$

In the last step (94), we used the expression in (14) for ρ. It can now be seen that, when $L\to\infty$, $P_{\mathrm{rx}}[n] \xrightarrow{\text{a.s.}} \bar{P}_{\mathrm{rx}}$ and the correlation goes to zero.

Appendix C
Proof of Theorem 1

We have seen how the estimated signal can be written as the sum of the following terms:

$$\begin{aligned}\hat{\mathbf{x}}_k[\nu] = \rho\sum_{k'=1}^{K}\sqrt{c_{k'}\beta_{k'}P_{k'}}\big(\alpha_{kk'}\mathbf{x}_k[\nu] + \mathbf{i}_{kk'}[\nu]\big) + \rho\mathbf{u}_k'[\nu]\\ + \rho\mathbf{z}_k'[\nu] + \mathbf{e}_k'[\nu]. \quad (96)\end{aligned}$$

It can be shown that each term in this sum is uncorrelated to the other terms. Most correlations are easy to show, except the correlation between the error due to quantization $\mathsf{e}'_k[\nu]$ and the transmit signal $\mathsf{x}_k[\nu]$. To show that this correlation is zero, we show that all the time-domain signals $\{e'_k[n]\}$ and $\{x_k[n]\}$ are pairwise uncorrelated if $x_k[n]$ is Gaussian. The procedure is similar to the proof of Lemma 3. We note that $x_k[n']$, $y_m[n]$, $e_m[n]$ form a Markov chain in that order. Therefore:

$$\begin{aligned}
&\mathbb{E}\big[e_m^*[n]x_k[n']\big] \\
&\quad= \mathbb{E}\Big[\mathbb{E}\big[e_m^*[n]x_k[n'] \mid y_m[n]\big]\Big] && (97)\\
&\quad= \mathbb{E}\Big[\mathbb{E}\big[e_m^*[n] \mid y_m[n]\big]\mathbb{E}\big[x_k[n'] \mid y_m[n]\big]\Big] && (98)\\
&\quad= \frac{\mathbb{E}[y_m^*[n]x_k[n']]}{\mathbb{E}[|y_m[n]|^2]}\mathbb{E}\big[(q_m^*[n]-\rho^* y_m^*[n])y_m[n]\big] && (99)\\
&\quad= \frac{\mathbb{E}[y_m^*[n]x_k[n']]}{\mathbb{E}[|y_m[n]|^2]}\Big(\mathbb{E}\big[q_m^*[n]y_m[n]\big]-\rho^*\mathbb{E}\big[|y_m[n]|^2\big]\Big) && (100)\\
&\quad= 0, && (101)
\end{aligned}$$

for all n and n'. In the last step, we used (14).

The variances of $\mathsf{u}'_k[\nu]$ and $\mathsf{z}'_k[\nu]$ are given by

$$\mathbb{E}\big[|\mathsf{u}'_k[\nu]|^2\big] = \mathbb{E}\big[|\mathsf{u}_m[\nu]|^2\big] = \sum_{k'=1}^{K}\beta_{k'}P_{k'}\big(1-c_{k'}\big), \quad (102)$$

$$\mathbb{E}\big[|\mathsf{z}'_k[\nu]|^2\big] = \mathbb{E}\big[|\mathsf{z}_m[\nu]|^2\big] = N_0, \quad (103)$$

By evaluating the expectations in the rate expression in (68), we obtain

$$\big|\mathbb{E}\big[\mathsf{x}_k^*[\nu]\hat{\mathsf{x}}_k[\nu]\big]\big|^2 \to \rho^2 c_k\beta_k P_k G_k, \quad (104)$$

$$\begin{aligned}
\mathbb{E}\big[|\hat{\mathsf{x}}_k[\nu]|^2\big] &\to \rho^2\Big(c_k\beta_k P_k G_k \\
&+ \sum_{k'=1}^{K}\big(c_k\beta_k P_k I_{kk'} + \beta_{k'}P_{k'}(1-c_{k'})\big) + N_0 + Q'\Big), \quad (105)
\end{aligned}$$

as $L\to\infty$. Here we used Corollary 1. Letting the number of channel taps $L\to\infty$ thus gives the rate $R'_k = \log_2(1+\mathsf{SINR}_k)$, where

$$\mathsf{SINR}_k = \frac{c_k\beta_k P_k G_k}{\sum_{k'=1}^{K}\big(c_k\beta_k P_k I_{kk'}+\beta_{k'}P_{k'}(1-c_{k'})\big)+N_0+Q'}. \quad (106)$$

REFERENCES

[1] R. H. Walden, "Analog-to-digital converter survey and analysis," *IEEE J. Sel. Areas Commun.*, vol. 17, no. 4, pp. 539–550, Apr. 1999.

[2] E. Björnson, M. Matthaiou, and M. Debbah, "Massive MIMO with non-ideal arbitrary arrays: Hardware scaling laws and circuit-aware design," *IEEE Trans. Wireless Commun.*, vol. 14, no. 8, pp. 4353–4368, Aug. 2015.

[3] J. Choi, J. Mo, and R. W. Heath, Jr., "Near maximum-likelihood detector and channel estimator for uplink multiuser massive MIMO systems with one-bit ADCs," *IEEE Trans. Commun.*, vol. 64, no. 5, pp. 2005–2018, May 2016.

[4] S. Jacobsson, G. Durisi, M. Coldrey, U. Gustavsson, and C. Studer. (Feb. 2016). "Throughput analysis of massive MIMO uplink with low-resolution ADCs." [Online]. Available: https://arxiv.org/abs/1602.01139

[5] J. Mo and R. W. Heath, Jr., "Capacity analysis of one-bit quantized MIMO systems with transmitter channel state information," *IEEE Trans. Signal Process.*, vol. 63, no. 20, pp. 5498–5512, Oct. 2015.

[6] C. Risi, D. Persson, and E. G. Larsson. (Apr. 2014). "Massive MIMO with 1-bit ADC." [Online]. Available: https://arxiv.org/abs/1404.7736

[7] N. Liang and W. Zhang, "Mixed-ADC massive MIMO," *IEEE J. Sel. Areas Commun.*, vol. 34, no. 4, pp. 983–997, Apr. 2016.

[8] M. T. Ivrlač and J. A. Nossek, "On MIMO channel estimation with single-bit signal-quantization," in *Proc. ITG Workshop Smart Antennas*, Feb. 2007.

[9] O. Dabeer and U. Madhow, "Channel estimation with low-precision analog-to-digital conversion," in *Proc. IEEE Int. Conf. Commun.*, May 2010, pp. 1–6.

[10] J. Mo, P. Schniter, N. González-Prelcic, and R. W. Heath, Jr., "Channel estimation in millimeter wave MIMO systems with one-bit quantization," in *Proc. Asilomar Conf. Signals, Syst. Comput.*, Nov. 2014, pp. 957–961.

[11] C. Rusu, R. Mendez-Rial, N. González-Prelcic, and R. W. Heath, Jr., "Adaptive one-bit compressive sensing with application to low-precision receivers at mmWave," in *Proc. IEEE Global Commun. Conf.*, Dec. 2015, pp. 1–6.

[12] C. Rusu, N. González-Prelcic, and R. W. Heath, Jr., "Low resolution adaptive compressed sensing for mmWave MIMO receivers," in *Proc. Asilomar Conf. Signals, Syst. Comput.*, Nov. 2015, pp. 1138–1143.

[13] C. Studer and G. Durisi, "Quantized massive MU-MIMO-OFDM uplink," *IEEE Trans. Commun.*, vol. 64, no. 6, pp. 2387–2399, Jun. 2016.

[14] S. Wang, Y. Li, and J. Wang, "Multiuser detection in massive spatial modulation MIMO with low-resolution ADCs," *IEEE Trans. Wireless Commun.*, vol. 14, no. 4, pp. 2156–2168, Apr. 2015.

[15] N. Liang and W. Zhang, "Mixed-ADC massive MIMO uplink in frequency-selective channels," *IEEE Trans. Commun.*, to be published. [Online]. Available: https://arxiv.org/abs/1601.02082

[16] T. L. Marzetta, "Noncooperative cellular wireless with unlimited numbers of base station antennas," *IEEE Trans. Wireless Commun.*, vol. 9, no. 11, pp. 3590–3600, Nov. 2010.

[17] J. Vieira *et al.*, "A flexible 100-antenna testbed for massive MIMO," in *Proc. IEEE Global Commun. Conf.*, Dec. 2014, pp. 287–293.

[18] C. Mollén, J. Choi, E. G. Larsson, and R. W. Heath, Jr., "One-bit ADCs in wideband massive MIMO systems with OFDM transmission," in *Proc. IEEE Int. Conf. Acoust., Speech Signal Process.*, Mar. 2016, pp. 3386–3390.

[19] L. Fan, S. Jin, C.-K. Wen, and H. Zhang, "Uplink achievable rate for massive MIMO systems with low-resolution ADC," *IEEE Commun. Lett.*, vol. 19, no. 12, pp. 2186–2189, Dec. 2015.

[20] J. Zhang, L. Dai, S. Sun, and Z. Wang, "On the spectral efficiency of massive MIMO systems with low-resolution ADCs," *IEEE Commun. Lett.*, vol. 20, no. 5, pp. 842–845, May 2016.

[21] C. Mollén, J. Choi, E. G. Larsson, and R. W. Heath, Jr., "Performance of linear receivers for wideband massive MIMO with one-bit ADCs," *Int. ITG Workshop Smart Antennas*, Munich, Germany, Mar. 2016, pp. 1–7.

[22] C. Mollén. (2016). *Achievable rate analysis for massive MIMO base stations with one-bit ADCs*. [Online]. Available: http://urn.kb.se/resolve?urn=urn:nbn:se:liu:diva-131957

[23] F. Kamgar, A. J. Rouphael, and M. Motamed, "LNA control-circuit for receive closed loop automatic gain control," U.S. Patent 6 324 387, Nov. 27, 2001,

[24] T. Cui and C. Tellambura, "Power delay profile and noise variance estimation for OFDM," *IEEE Commun. Lett.*, vol. 10, no. 1, pp. 25–27, Jan. 2006.

[25] *3rd Generation Partnership Project; Technical Specification Group Radio Access Network; Evolved Universal Terrestrial Radio Access (E-UTRA); Base Station (BS) Conformance Testing (Release 10)*, document 3GPP TS36.141, 2011.

[26] R. Narasimha, M. Lu, N. R. Shanbhag, and A. C. Singer, "BER-optimal analog-to-digital converters for communication links," *IEEE Trans. Signal Process.*, vol. 60, no. 7, pp. 3683–3691, Jul. 2012.

[27] T. Koch and A. Lapidoth, "At low SNR, asymmetric quantizers are better," *IEEE Trans. Inf. Theory*, vol. 59, no. 9, pp. 5421–5445, Sep. 2013.

[28] W. Feller, *An Introduction to Probability Theory and Its Applications*, vol. 1, 3rd ed. New York, NY, USA: Wiley, 1968,

[29] J. Max, "Quantizing for minimum distortion," *IRE Trans. Inf. Theory*, vol. 6, no. 1, pp. 7–12, Mar. 1960.

[30] Q. Bai and J. A. Nossek, "Energy efficiency maximization for 5G multi-antenna receivers," *Trans. Emerg. Telecommun. Technol.*, vol. 26, no. 1, pp. 3–14, Jan. 2015.

[31] C. Mollén, E. G. Larsson, and T. Eriksson, "Waveforms for the massive MIMO downlink: Amplifier efficiency, distortion and performance," *IEEE Trans. Commun.*, to be published.

[32] M. Medard, "The effect upon channel capacity in wireless communications of perfect and imperfect knowledge of the channel," *IEEE Trans. Inf. Theory*, vol. 46, no. 3, pp. 933–946, May 2000.

[33] B. M. Hochwald, T. L. Marzetta, and V. Tarokh, "Multiple-antenna channel hardening and its implications for rate feedback and scheduling," *IEEE Trans. Inf. Theory*, vol. 50, no. 9, pp. 1893–1909, Sep. 2004.
[34] H. Yang and T. L. Marzetta, "Performance of conjugate and zero-forcing beamforming in large-scale antenna systems," *IEEE J. Sel. Areas Commun.*, vol. 31, no. 2, pp. 172–179, Feb. 2013.
[35] A. Pitarokoilis, S. K. Mohammed, and E. G. Larsson, "On the optimality of single-carrier transmission in large-scale antenna systems," *IEEE Wireless Commun Lett.*, vol. 1, no. 4, pp. 276–279, Apr. 2012.
[36] N. Jindal, "MIMO broadcast channels with finite-rate feedback," *IEEE Trans. Inf. Theory*, vol. 52, no. 11, pp. 5045–5060, Nov. 2006.
[37] P. Ding, D. J. Love, and M. D. Zoltowski, "Multiple antenna broadcast channels with shape feedback and limited feedback," *IEEE Trans. Signal Process.*, vol. 55, no. 7, pp. 3417–3428, Jul. 2007.
[38] A. J. Viterbi and J. K. Omura, *Principles of Digital Communication and Coding*. New York, NY, USA: McGraw-Hill, 1979.
[39] A. Mezghani and J. A. Nossek, "On ultra-wideband MIMO systems with 1-bit quantized outputs: Performance analysis and input optimization," in *Proc. IEEE Int. Symp. Inform. Theory*, Jun. 2007, pp. 1286–1289.

Christopher Mollén received the M.Sc. degree in 2013 and the Licentiate of Engineering degree in 2016 from Linköping University, Sweden, where he is currently pursuing the Ph.D. degree with the Department of Electrical Engineering, Division for Communication Systems. Prior to his Ph.D. studies, he has worked as intern at Ericsson in Kista, Sweden, and in Shanghai, China. From 2011 to 2012, he studied at the Eidgenössische Technische Hochschule (ETH) Zürich, Switzerland, as an exchange student in the Erasmus Programme. From 2015 to 2016, he visited the University of Texas at Austin as a Fulbright Scholar. His research interest is low-complexity hardware implementations of massive MIMO base stations, including low-PAR precoding, low-resolution ADCs, and nonlinear amplifiers.

Junil Choi received the B.S. (Hons.) and M.S. degrees in electrical engineering from Seoul National University in 2005 and 2007, respectively, and the Ph.D. degree in electrical and computer engineering from Purdue University in 2015. From 2007 to 2011, he was a Member of Technical Staff with the Samsung Advanced Institute of Technology and Samsung Electronics Company Ltd., South Korea, where he was involved in advanced codebook and feedback framework designs for the 3GPP LTE/LTE-Advanced and the IEEE 802.16m standards. He was a Post-Doctoral Fellow with The University of Texas at Austin. He is currently with the Department of Electrical Engineering, Pohang University of Science and Technology, as an Assistant Professor. His research interests are in the design and analysis of massive MIMO, mmWave communication systems, distributed reception, and vehicular communication systems.

Dr. Choi was a co-recipient of the 2015 IEEE Signal Processing Society Best Paper Award, the 2013 Global Communications Conference (GLOBECOM) Signal Processing for Communications Symposium Best Paper Award, and the 2008 Global Samsung Technical Conference Best Paper Award. He received the Michael and Katherine Birck Fellowship from Purdue University in 2011, the Korean Government Scholarship Program for Study Overseas from 2011 to 2013, the Purdue University ECE Graduate Student Association Outstanding Graduate Student Award in 2013, and the Purdue College of Engineering Outstanding Student Research Award in 2014.

Erik G. Larsson (S'99–M'03–SM'10–F'16) received the Ph.D. degree from Uppsala University, Sweden, in 2002. He was with the Royal Institute of Technology, Stockholm, Sweden, the University of Florida, Gainesville, FL, USA, The George Washington University, Washington, DC, USA, and Ericsson Research, Sweden. In 2015, he was a Visiting Fellow with Princeton University, Princeton, NJ, USA for four months. He is currently a Professor of Communication Systems with Linköping University, Linköping, Sweden.

His main professional interests are within the areas of wireless communications and signal processing. He has co-authored some 130 journal papers on these topics, he is co-author of the two textbooks *Space-Time Block Coding for Wireless Communications* (Cambridge University Press, 2003) and *Fundamentals of Massive MIMO* (Cambridge University Press, 2016). He is co-inventor on 16 issued and many pending patents on wireless technology.

He serves as the Chair of the IEEE Signal Processing Society SPCOM Technical Committee from 2015 to 2016 and he served as the Chair of the Steering Committee of the IEEE WIRELESS COMMUNICATIONS LETTERS from 2014 to 2015. He was the General Chair of the Asilomar Conference on Signals, Systems and Computers in 2015, and the Technical Chair in 2012. He served as an Associate Editor of the IEEE TRANSACTIONS ON COMMUNICATIONS from 2010 to 2014 and the IEEE TRANSACTIONS ON SIGNAL PROCESSING from 2006 to 2010.

Dr. Larsson received the IEEE Signal Processing Magazine Best Column Award twice, in 2012 and 2014, and the IEEE ComSoc Stephen O. Rice Prize in Communications Theory in 2015.

Robert W. Heath, Jr. (S'96–M'01–SM'06–F'11) received the B.S. and M.S. degrees from the University of Virginia, Charlottesville, VA, USA, in 1996 and 1997, respectively, and the Ph.D. degree from Stanford University, Stanford, CA, USA, in 2002, all in electrical engineering. From 1998 to 2001, he was a Senior Member of the Technical Staff and a Senior Consultant with Iospan Wireless Inc., San Jose, CA, where he was involved in the design and implementation of the physical and link layers of the first commercial MIMO-OFDM communication system. Since 2002, he has been with the Department of Electrical and Computer Engineering, The University of Texas at Austin, where he is Cullen Trust for Higher Education Endowed Professor, and a Member of the Wireless Networking and Communications Group. He is also the President and the CEO of MIMO Wireless Inc. He has co-authored the books *Millimeter Wave Wireless Communications* (Prentice Hall, 2014) and *Digital Wireless Communication: Physical Layer Exploration Lab Using the NI USRP* (National Technology and Science Press, 2012).

Dr. Heath is an elected member of the Board of Governors of the IEEE Signal Processing Society, a licensed amateur radio operator, a private pilot, and a Registered Professional Engineer in Texas. He was a Distinguished Lecturer in the IEEE Signal Processing Society. He is an ISI Highly Cited Researcher. He has been a Co-Author of several best paper awards, including the 2010 and 2013 *EURASIP Journal on Wireless Communications and Networking* Best Paper Awards, the 2012 *Signal Processing Magazine* Best Paper Award, the 2013 Signal Processing Society Best Paper Award, the 2014 *EURASIP Journal on Advances in Signal Processing* Best Paper Award, the 2014 *Journal of Communications and Networks* Best Paper Award, the 2016 IEEE Communications Society Fred W. Ellersick Prize, and the 2016 IEEE Communications and Information Theory Societies Joint Paper Award.